

# EFFECTS OF Ni CONTENT ON THE MICROSTRUCTURE AND MECHANICAL PROPERTIES OF ALUMINA/SILICON CARBIDE TOOL COMPOSITES

## VPLIV VSEBNOSTI NIKLJA NA MIKROSTRUKTURO IN MEHANSKE LASTNOSTI KOMPOZITOV NA OSNOVI $\text{Al}_2\text{O}_3/\text{SiC}$ ZA REZALNA ORODJA

Tingting Liao<sup>1,2</sup>, Xiaoya Shen<sup>1</sup>, Fanchang Kong<sup>3</sup>, XinYi Yang<sup>1</sup>, Ruotong Tian<sup>1</sup>, Lin He<sup>1</sup>, Chenyang Zhu<sup>1</sup>, Biao Guo<sup>4</sup>, Pingping Liu<sup>1</sup>, Jiehui Liu<sup>1\*</sup>, Xi Zhang<sup>2\*</sup>

<sup>1</sup>School of Materials and Environmental Engineering, Chengdu Technological University, Chengdu, Sichuan, 611730, China

<sup>2</sup>School of Materials Science and Engineering, Southwest Jiaotong University, Chengdu, Sichuan, 610031, China

<sup>3</sup>CRRC Tangshan Co., Ltd, Tangshan, Hebei, 064099, China

<sup>4</sup>Key Laboratory of materials and surface technology (Ministry of Education), School of Materials Science and Engineering, Xihua University, Chengdu, Sichuan, 610039, China

*Prejem rokopisa – received: 2024-09-26; sprejem za objavo – accepted for publication: 2025-02-04*

doi:10.17222/mit.2024.1286

Alumina-based ceramic composites are widely used for cutting tools owing to their high strength and oxidation resistance. However, their brittle nature and low toughness adversely affect their use and performance. In this study, alumina/silicon carbide ( $\text{Al}_2\text{O}_3/\text{SiC}$ ) composites with different mass fractions of Ni (5 %, 10 %, 15 %, and 20 %) were prepared via vacuum hot-press sintering to optimise their strength and toughness. The structural and mechanical properties of the composites were characterised using various techniques. The hardness and bending strength of the Ni-doped  $\text{Al}_2\text{O}_3/\text{SiC}$  composites increased with the Ni content up to 10 % and decreased with a further increase in the Ni content. The maximum values of the hardness, bending strength, and fracture toughness were 7.19 GPa, 871.25 MPa, and  $7.90 \text{ MPa}\cdot\text{m}^{1/2}$ , respectively. Thus, the addition of Ni improved the mechanical properties overall and provided a toughening effect.

Keywords: Nickel, ceramic composite, toughness

Keramični kompoziti na osnovi aluminijevega oksida se veliko uporabljajo za rezalna orodja, ker imajo visoko trdnost in odpornost proti oksidaciji pri visokih temperaturah. Vendar pa zaradi njihove naravne krhkosti in nizke žilavosti niso dovolj učinkoviti. V tem članku avtorji opisujejo študijo kompozitov na osnovi  $\text{Al}_2\text{O}_3/\text{SiC}$  z različnim masnim deležem dodatka Ni. Avtorji so pripravili kompozite s 5 %, 10 %, 15 %, in 20 % Ni s postopkom vakumskega vročega sintranja pod tlakom, da bi optimizirali njihovo trdnost in žilavost. Sledila je strukturna in mehanska karakterizacija izdelanih kompozitov z različnimi tehnikami. Trdota in upogibna trdnost z Ni dopiranih  $\text{Al}_2\text{O}_3/\text{SiC}$  kompozitov je naraščala z vsebnostjo dodanega Ni do 10 % in nato je začela počasi padati z nadaljnjim naraščanjem vsebnosti Ni. Optimalne dosežene vrednosti trdote, upogibne trdnosti in lomne žilavosti pri dodatku 10 % Ni so bile 7,19 GPa, 871,25 MPa in  $7,90 \text{ MPa}\cdot\text{m}^{1/2}$ . Na ta način so avtorji dokazali, da je z dodatkom niklja možno izboljšati žilavost te vrste keramičnih kompozitov.

Ključne besede: nikelj, keramični kompozit, žilavost

## 1 INTRODUCTION

Alumina ( $\text{Al}_2\text{O}_3$ )-based ceramic cutting tools are widely used owing to their high mechanical strength and oxidation/high-temperature resistance, chemical stability, and cost-effectiveness. However, the high brittleness and low toughness of  $\text{Al}_2\text{O}_3$  affect their performance and reliability. To improve the performance of ceramic materials,<sup>1,2</sup> toughening methods such as particle-dispersion toughening, whisker toughening, phase-change toughening, and synergistic toughening have been explored.<sup>3</sup> Zhu et al.<sup>4</sup> studied zirconia-toughened  $\text{Al}_2\text{O}_3$  ceramics and reported that samples sintered at 1650 °C with a relative density of 96.65 % exhibited the best mechanical perfor-

mance, with a flexural strength of 572.0 MPa, Vickers hardness of 16.2 GPa, and fracture toughness of  $7.4 \text{ MPa}\cdot\text{m}^{1/2}$ . Such ceramics have excellent mechanical properties, giving them considerable potential for dental applications. Chin et al.<sup>5</sup> examined the interactions between crack deflection and plastic deformation in  $\text{Al}_2\text{O}_3/\text{Ti}_3\text{SiC}_2$  and found that the toughening effect stemmed mainly from crack deflection.

Among these toughened alumina ceramics, silicon carbide (SiC)-reinforced  $\text{Al}_2\text{O}_3$  matrix composites exhibit outstanding mechanical properties. The particle bridging at the crack tip and the change in fracture mode caused by residual stress and crack deflection are the primary strengthening and toughening mechanisms.<sup>6</sup> Moreover, transgranular SiC particles undergo less shrinkage than the surrounding matrix and provide a hydrostatic "expansion" effect in the core of each  $\text{Al}_2\text{O}_3$  grain. Such grain expansion tightens the internal  $\text{Al}_2\text{O}_3$  grain bound-

\*Corresponding author's e-mail:

ljhui1@cdtu.edu.cn (Jiehui Liu)



© 2025 The Author(s). Except when otherwise noted, articles in this journal are published under the terms and conditions of the Creative Commons Attribution 4.0 International License (CC BY 4.0).

aries, shielding both the weakly bonded and unbonded (cracked) grain boundaries.<sup>7</sup>

However, the toughening effect of Al<sub>2</sub>O<sub>3</sub>/SiC remains limited. The addition of different types of particles to Al<sub>2</sub>O<sub>3</sub>/SiC composites can further increase their toughness and bending strengths.<sup>8–11</sup> Ni is a useful metal that is added to improve the fracture toughness. Gustafsson et al.<sup>12</sup> reported that the addition of Ni in Al<sub>2</sub>O<sub>3</sub>-based materials prepared via *in situ* reactions resulted in the formation of dispersed Ni phases at the grain boundaries, which increased the strength and toughness of these materials. Moreover, the incorporation of Ni impedes the grain growth, increasing the hardness and wear resistance of composite materials. Wu et al.<sup>13</sup> researched self-lubricating cutting tools that contained Ni-coated hexagonal boron nitride and reported that a tool with a Ni coating had better densification, wear resistance, and cutting performance than an uncoated tool, as well as superior mechanical properties.

In Al<sub>2</sub>O<sub>3</sub>-based composite materials, Ni is typically present as a dispersed phase between the matrix and grain boundaries. Studies have demonstrated that an optimal amount of Ni can refine the grain structure, improving both the material strength and hardness. For instance, when Ni is incorporated into Al<sub>2</sub>O<sub>3</sub>/SiC composites via an *in-situ* reaction, the formation of Ni particles at the grain boundaries effectively immobilises the Al<sub>2</sub>O<sub>3</sub>/SiC, impeding the grain growth and consequently enhancing the flexural strength and fracture toughness.<sup>14</sup> Martínez et al.<sup>15</sup> reported the outstanding mechanical properties of particle-reinforced Ni–alumina metal matrix nanocomposites. After 10 h of milling, the Al<sub>2</sub>O<sub>3</sub> nanoparticles were well-dispersed in the Ni matrix, reinforcing the composites. Firoozbakht et al.<sup>16</sup> researched Al<sub>2</sub>O<sub>3</sub>-SiC-Ni nanocermet in an air environment and found that the microstructure of sintered samples consisted of a continuous Ni network surrounding Al<sub>2</sub>O<sub>3</sub> grains, with no structural defects or Ni oxidation.

The Ni toughening mechanism is effective, but does not fully explain the toughening of the tool composites. To improve the mechanical performance of ceramic tool composites, we prepared Ni-doped Al<sub>2</sub>O<sub>3</sub>/SiC composites via hot-press sintering. We then studied the effects of the Ni content on their mechanical properties to clarify the mechanism of metal toughening in multiphase ceramics.

## 2 EXPERIMENTAL PART

High-purity powders of Al<sub>2</sub>O<sub>3</sub>, SiC, and Ni were obtained from Yijia Metal Products Co., Ltd. (Jiaxing, China), and Al<sub>2</sub>O<sub>3</sub> with 5 % SiC (mass fraction) was used as the base material. The Ni powders were added in mass fractions of 5 %, 10 %, 15 %, and 20 % to prepare the composite materials. The physical properties of the

raw materials are presented in **Table 1**, and the compositions of the prepared samples are presented in **Table 2**.

**Table 1:** Properties of the raw materials

Material	Molecular weight (g/mol)	Purity (%)	Particle size (μm)
Al <sub>2</sub> O <sub>3</sub>	101.96	99.99	65
SiC	40.1	99.99	65
Ni	58.69	99.99	65

**Table 2:** Compositions of the different samples (g)

Samples (with different Ni contents)	Al <sub>2</sub> O <sub>3</sub>	SiC	Ni	Gross weight
0 % Ni	95	5	0	100
5 % Ni	90	5	5	100
10 % Ni	85	5	10	100
15 % Ni	80	5	15	100
20 % Ni	75	5	20	100

A planetary ball mill (XQM-4-KL, China) was used to mix the powder samples, with ethanol and Al<sub>2</sub>O<sub>3</sub> balls as the milling media. The ball-milling speed was 250 min<sup>-1</sup>, and the duration of milling was 5 h. The composite materials with different Ni contents were prepared via vacuum hot-press sintering (VHP140/25-2300, China) at 1400 °C and 40 MPa with a heating rate of 10 °C/min and a holding time for sintering of 60 min. Their structures were characterised using X-ray diffraction (XRD; TD-3500, China) with a scanning speed of 6°/min, scanning range of 0°–90°, step size of 0.04°, and sampling time of 0.4 s. The actual densities ( $\rho_1$ ) of the samples were measured using a density tester (AR-150ME, China). The theoretical densities ( $\rho_2$ ) were calculated from the theoretical densities of Al<sub>2</sub>O<sub>3</sub>, SiC, and Ni, and the relative densities ( $\rho$ ) were calculated using the following equation.

$$\rho = \rho_1 \rho_2 \quad (1)$$

The microhardnesses of the composite materials were evaluated using a Vickers hardness tester (HXD-100TM/LCD, China) under a load of 9.8 N for a duration of 15 s. The bending strength was determined via three-point tests using a universal testing machine (WDW-2.0, China). The sample size was 30 mm × 4 mm × 3 mm. The crossbeam speed of the testing machine was set to 0.5 mm/min, and the bending strength was calculated as follows:

$$\sigma = \frac{3FL}{2bd^2} \quad (2)$$

where  $L$  represents the lower span of the fixture,  $b$  represents the width of the sample (4 mm), and  $d$  represents the height of the sample (3 mm). Scanning electron microscopy (SEM; HITACHI S-3400, Japan) was used to characterise the fracture sections of the bent specimens. The fracture toughness of the material was measured via micro-Vickers hardness tester (HVS-30, China) at a load

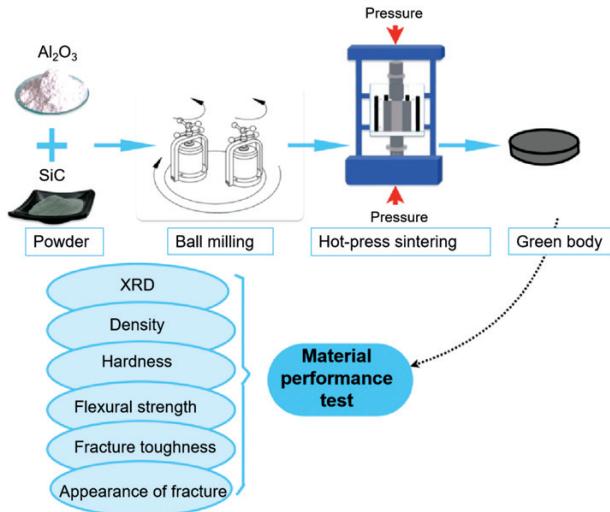


**Figure 1:** Preparation and characterization of Ni-doped Al<sub>2</sub>O<sub>3</sub>/SiC composites

of 294 N, which was held for 30 s. It was calculated as follows:

$$K_{IC} = \beta \cdot \left( \frac{E}{H} \right)^{1/2} \left( \frac{F}{C^{3/2}} \right) \quad (3)$$

where  $K_{IC}$  represents the fracture toughness,  $\beta$  is the test constant (0.016),  $E$  represents the Young's modulus of the material (in GPa),  $H$  represents the Vickers hardness of the material (in GPa),  $F$  represents the acting load of the Vickers hardness indentation (in N), and  $C$  represents the average indentation-crack radius (in mm).

In this study, One-way ANOVA was conducted using the IBM SPSS Statistics 19 software, with results presented as the mean  $\pm$  standard error ( $n = 3$ ). For statistical significance, a p-value threshold of less than 0.05 was adopted. In the graphical representations, extremely significant differences ( $p < 0.001$ ), highly significant differences ( $p < 0.01$ ), and significant differences ( $p < 0.05$ ) are denoted by \*\*\*, \*\*, and \*, respectively.

### 3 RESULTS AND DISCUSSION

#### 3.1 Structure

**Figure 2** shows the XRD patterns of the Al<sub>2</sub>O<sub>3</sub>/SiC composites prepared with different Ni contents. All the samples exhibit characteristic peaks for standard Al<sub>2</sub>O<sub>3</sub>. The main peaks are at 25°, 35°, 38°, 44°, 53°, 57°, 66°, and 68°, indicating that the addition of Si, C, Ni did not affect the peak intensity of Al<sub>2</sub>O<sub>3</sub>. Furthermore, the peak at 45° corresponding to Ni was observed in the samples with Ni contents of 10–20 w/%. The intensity of the Ni diffraction peak increased with the Ni content. In addition, peaks corresponding to metallic Ni and Ni compounds, such as Ni(CO)<sub>4</sub> at 46°, were observed for the samples with high Ni contents (10 %, 15 %, and 20 %), accompanied by small peaks nearby. At 1400 °, Ni is semi-molten, most of the peak sites (Al<sub>2</sub>O<sub>3</sub>-related peak

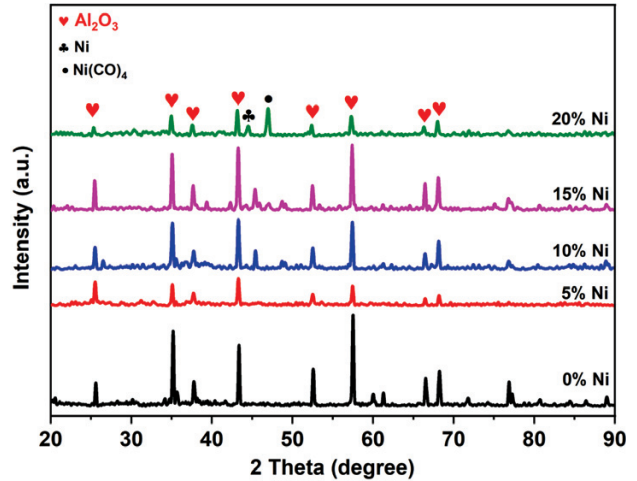


**Figure 2:** XRD patterns of Al<sub>2</sub>O<sub>3</sub>/SiC composites with different Ni contents

locations) in the samples are similar, and the reactions between Ni and Al<sub>2</sub>O<sub>3</sub> are thought to mainly occur in the first atomic layer of the interface<sup>17</sup>. Fluctuant peaks at 44–50° suggest that the chemical reaction produces Ni compounds at high temperatures. Most of the Al<sub>2</sub>O<sub>3</sub>-related peaks and Ni-related peaks at 45° reported by Wang et al.<sup>18</sup> were similar. Ni was present as a single phase in the composite materials, and it also reacted with Al and O<sup>19</sup>. These results indicated that Ni was successfully added as a single phase or a dispersion in the composites.

#### 3.2 Relative density

The density of the Al<sub>2</sub>O<sub>3</sub>/SiC composite without the addition of Ni (0 %) was measured as 95.24 %, and it increased with the Ni content (Figure 3). The density of the composite reached 98.00 % at 15 % Ni. The increase in the density is attributed to the filling of the gaps between the Al<sub>2</sub>O<sub>3</sub> and SiC particles by the Ni particles<sup>20,21</sup>.

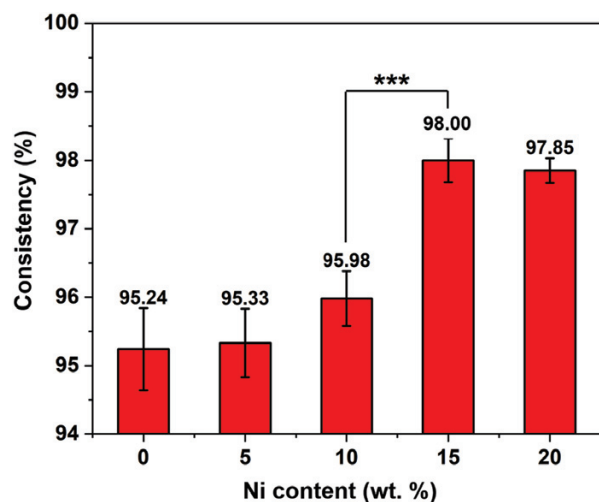


**Figure 3:** Densities of Al<sub>2</sub>O<sub>3</sub>/SiC composites with different Ni contents

The wetting effect of Ni between alumina and SiC reduces the interfacial energy between particles, which facilitates the rearrangement and compact stacking of particles, increasing the density.<sup>22,23</sup> This strengthens the bonding between the particles after sintering. With an increase in the Ni content, more gaps are filled, and the density increases.

### 3.3 Hardness

As shown in **Figure 4**, the hardness of the  $\text{Al}_2\text{O}_3/\text{SiC}$  composite material increases from 6.25 GPa (0 % Ni) to a maximum of 7.25 GPa with the addition of 10 % Ni. With a further increase in the Ni content, the hardness of the composite decreases (e.g., 5.9 GPa at 20 % Ni). As the relative density increases with the Ni content, atoms exhibit a higher degree of compactness in their arrangement.<sup>24</sup> The hardness shows a trend similar to that of the relative density with the addition of 5 % and 10 % Ni. However, when the Ni content surpasses a critical threshold, it may exceed the solubility limit in the matrix metal, resulting in the excessive precipitation of Ni or the formation of coarse intermetallic compounds within the brittle phases<sup>25</sup>. These coarse secondary phases not only fail to effectively enhance the hardness but can also compromise the overall mechanical properties of the material, reducing the hardness. Our results indicated that the hardness first increased and then decreased and that the  $\text{Al}_2\text{O}_3/\text{SiC}$  composites with 15 % Ni had the highest hardness.

### 3.4 Flexural strength

**Figure 5** presents the flexural strengths of the  $\text{Al}_2\text{O}_3/\text{SiC}$  composites with different Ni contents. Similar to the trend in hardness, with an increase in the Ni content, the flexural strength of the composites first increased and then decreased. When the Ni content was 15 %, the flexural strength of the  $\text{Al}_2\text{O}_3/\text{SiC}$  composite

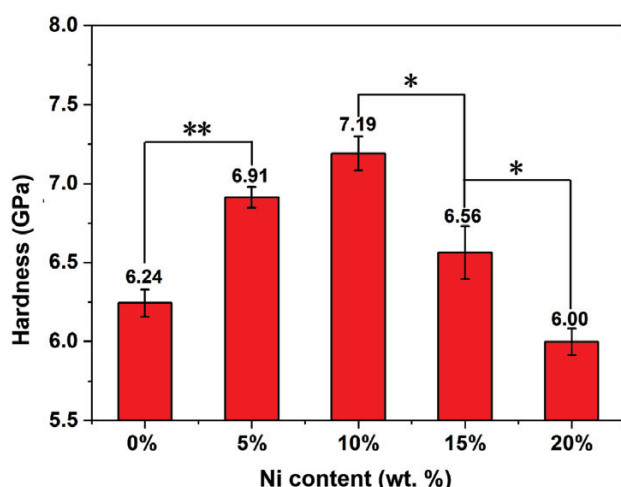


**Figure 4:** Hardnesses of the  $\text{Al}_2\text{O}_3/\text{SiC}$  composites with different Ni contents

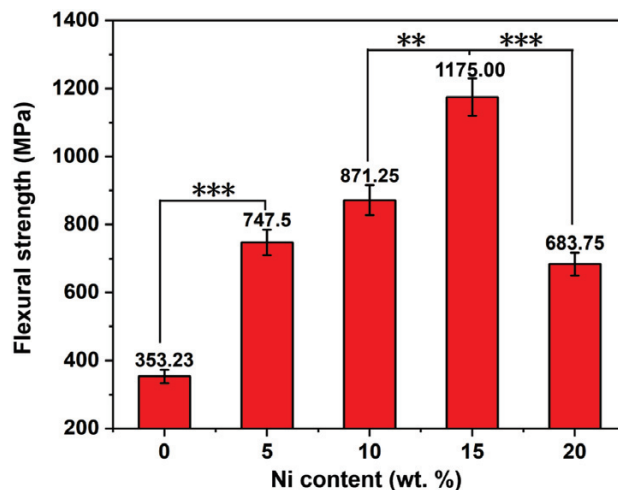


**Figure 5:** Flexural strengths of the  $\text{Al}_2\text{O}_3/\text{SiC}$  composites with different Ni contents

reached a maximum of approximately 1175.00 MPa. The addition of Ni may enhance the interface bonding, and the cementing action increases the flexural strength. The phase structure of the material may undergo changes with a further increase in Ni content, resulting in an excess of brittle phases or secondary phases<sup>15</sup>, which increases the brittleness of the material.

### 3.5 Fracture toughness

As shown in **Figure 6**, the fracture toughness of the  $\text{Al}_2\text{O}_3/\text{SiC}$  composite ( $6.63 \text{ MPa}\cdot\text{m}^{1/2}$ ) increases to a maximum of  $7.9 \text{ MPa}\cdot\text{m}^{1/2}$  at 10 % Ni and then decreases with a further increase in the Ni content. Thus, the addition of 5 %–10 % Ni increase the fracture toughness of the  $\text{Al}_2\text{O}_3/\text{SiC}$  composite ceramics. Ni, being a metal, exhibits high ductility and plasticity. The presence of the Ni phase within the ceramic matrix effectively impedes the crack propagation during the cracking process and

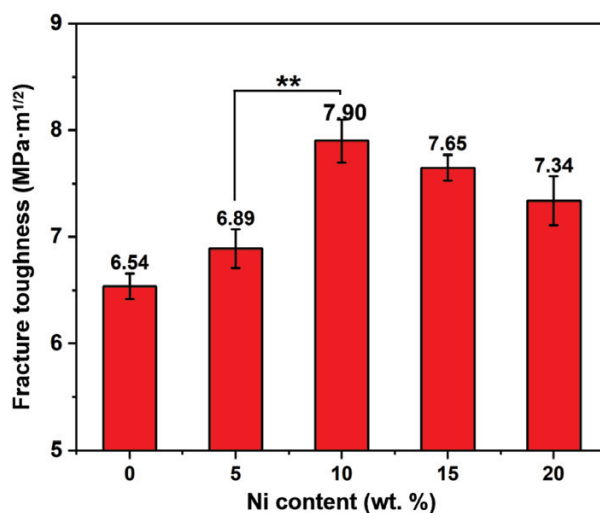


**Figure 6:** Fracture toughnesses of the  $\text{Al}_2\text{O}_3/\text{SiC}$  composites with different Ni contents



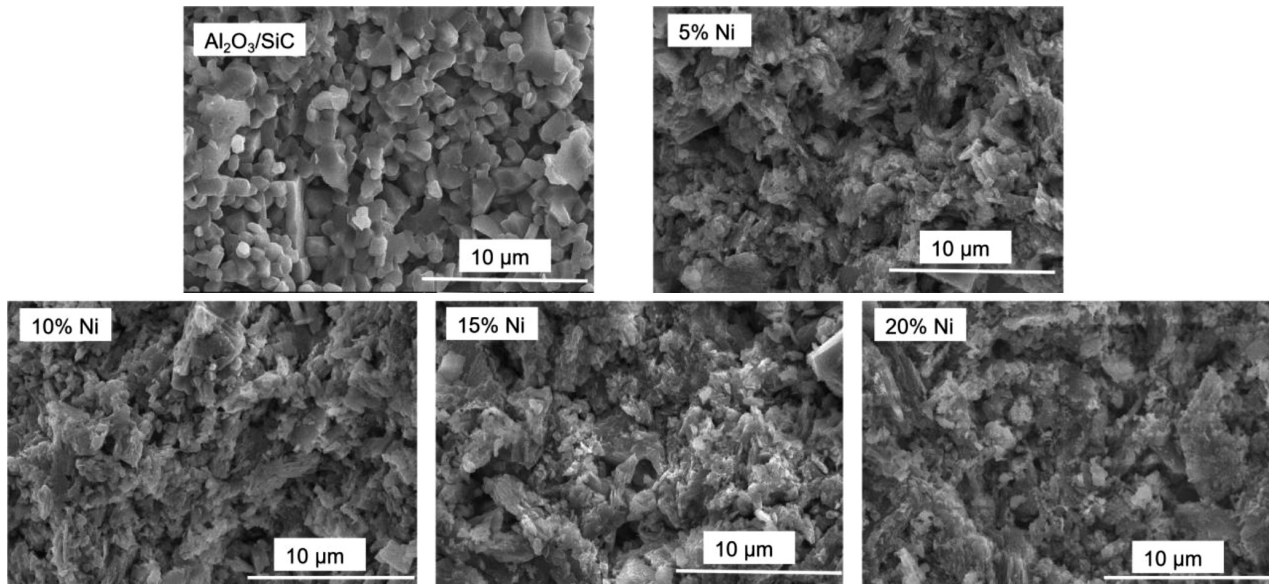


Figure 7: SEM images of the fracture surfaces of  $\text{Al}_2\text{O}_3/\text{SiC}$  composites with different Ni contents

increases the energy required for crack expansion,<sup>26,27</sup> which contributes to the fracture toughness. Additionally, the plastic deformation of the Ni enables the absorption of the energy required for crack propagation,<sup>28,29</sup> further increasing the fracture toughness. When the content exceeds 10 %, the fracture toughness of the  $\text{Al}_2\text{O}_3/\text{SiC}$  composite material decreases. On one hand, the strength of the interfacial bond between the Ni and alumina may be compromised due to excessive Ni content. High levels of Ni can destabilize or weaken the interfacial bond, leading to an increased likelihood of crack propagation at the interface, thereby reducing fracture toughness. On the other hand, the distribution and morphology of the Ni particles at high concentrations may induce stress concentration. If the Ni particles are unevenly distributed or form large agglomerates within the  $\text{Al}_2\text{O}_3$  matrix, these regions can become stress-concentration points, further diminishing the overall toughness of the material.

### 3.6 Fracture morphology

Figure 7 shows SEM images of the fractured sections of the different composites. Long columnar crystals can be observed in the pure  $\text{Al}_2\text{O}_3/\text{SiC}$  composites, and regular grain boundaries indicate the mode of intergranular fracture. However, the Ni-doped  $\text{Al}_2\text{O}_3/\text{SiC}$  composites exhibit smaller grains with obvious directional arrangement and grain-pulling holes. The addition of a metal element inhibits the grain growth, which results in grain refinement. Meanwhile, an indistinct grain boundary indicates transgranular fracture. Furthermore, the metal particles act as deflection or bridging agents<sup>30</sup> that result in crack deflection and interlocking, toughening the composite material.

According to the literature,<sup>31–33</sup> the grain size of the alumina decreases with an increase in its Ni content. When an Ni-doped  $\text{Al}_2\text{O}_3/\text{SiC}$  composite is sintered at a high temperature, the Ni melts and fills the gap between the  $\text{Al}_2\text{O}_3$  and SiC particles, increasing the density of the material and suppressing the crack formation. In this study, the fracture mode of the composite with 5 % Ni was almost completely intergranular fracture, with little transgranular fracture. However, with an increase in the Ni content, the fracture mode changed from intergranular to transgranular, indicating that the addition of Ni can strengthen the grain boundaries of  $\text{Al}_2\text{O}_3$  grains, hinder intergranular crack growth, and improve the mechanical properties of the material. Cracks propagate extensively within the grain interior, leading to elongated fracture paths and increased energy consumption. This mode of transgranular fracture necessitates overcoming robust intergranular bonding forces, with an increased fracture toughness.

When a small amount of Ni is added, the sintering activity of the material is improved, the sintering temperature is reduced, and the growth of  $\text{Al}_2\text{O}_3$  particles<sup>34</sup> is inhibited. This results in grain refinement and grain-boundary strengthening.<sup>35</sup> With an increase in the Ni content to a certain limit, enhanced grain refinement and grain-boundary strengthening can be achieved. After the high-temperature sintering of the  $\text{Al}_2\text{O}_3/\text{SiC}$  composite material, Ni no longer exists in the form of a single phase in the composite material; the reaction produces Ni-containing compounds, which are embedded in the  $\text{Al}_2\text{O}_3/\text{SiC}$  composite material and enhance its performance.<sup>36,37</sup>

At higher contents, Ni agglomerates and grows into larger particles. These particles impede grain-boundary movement, improving the grain connectivity.<sup>38</sup> Under the effect of an external load, stress concentration around

these particles<sup>39</sup> results in microcracks and expansion that can lead to fracture of the material. Thus, the mechanical properties of the Al<sub>2</sub>O<sub>3</sub>/SiC material are weakened at high Ni contents.

#### 4 CONCLUSIONS

Al<sub>2</sub>O<sub>3</sub>/SiC composites with different Ni contents were prepared via vacuum hot-press sintering. The following conclusions are drawn:

When the mass fraction of Ni is increased from 0 % to 15 %, the bonding effect of Ni is enhanced, and the density of Al<sub>2</sub>O<sub>3</sub>/SiC composite ceramics increases. When the Ni content is increased to 20 %, Ni agglomerates and becomes unevenly distributed in the material, reducing the density, strength, and toughness of the material.

With an increase in the Ni content, the hardness and bending strength of the Al<sub>2</sub>O<sub>3</sub>/SiC composite first increase and then decrease. The highest hardness is obtained when the Ni mass fraction is 10 %, and the bending strength is maximised at 15 % Ni.

When the mass fraction of Ni is 10 %, the hardness, bending strength, and fracture toughness are 7.19 GPa, 871.25 MPa, and 7.90 MPa·m<sup>1/2</sup>, respectively, i.e., the comprehensive mechanical properties of Al<sub>2</sub>O<sub>3</sub>/SiC are best at 10 % Ni.

In summary, the addition of Ni increased the density and comprehensively enhanced the mechanical properties of the Al<sub>2</sub>O<sub>3</sub>/SiC composite material by functioning as a reinforcing and toughening agent. Thus, the addition of metals to ceramic composite materials can improve their performance, which provides a new direction for the development of composites for Al<sub>2</sub>O<sub>3</sub>/SiC tools.

#### Acknowledgements

This research was sponsored by the Funds of National College Students Innovation and Entrepreneurship Training Program (202411116018), Sichuan Natural Science Foundation (2023NSFSC0870), and the Key Laboratory of Materials and Surface Technology, Ministry of Education (No. xxx-2024-yb006).

#### 5 REFERENCES

- P. S. Lu, H. Chen, J. J. Zhang, G. C. Xiao, M. D. Yi, Z. Q. Chen, C. H. Xu, Effects of graphene pull-out on the interfacial mechanical properties of alumina/graphene nanocomposite ceramic tool materials: Molecular dynamics analysis and material preparation[J]. *International Journal of Applied Ceramic Technology*, 21 (2023), 1, 451–464. doi:10.1111/ijac.14525
- P. Jurci, J. Bohovicová, M. Hudáková, P. Bílek, Characterization and wear performance of CrAgN thin films deposited on Cr-V ledeburitic tool steel[J]. *Mater. Tehnol.*, 48 (2014) 2, 159–170.
- A. Z. Wang, C. Ramírez, C. S. Wstts, O. Borrero-López, A. L. Ortiz, B. W. Sheldon, N. P. Padture, Fracture, fatigue, and sliding-wear behavior of nanocomposites of alumina and reduced graphene-oxide. *Acta Materialia*, 186 (2020), 29–39. doi:10.1016/j.actamat.2019.12.035
- L. Zhu, Y. D. Xu, S. W. Liu, H. H. Chen, J. Y. Tao, X. Tong, Y. C. Li, S. B. Huang, J. X. Lin, C. Wen, J. F. Ma, Microstructure, mechanical properties, friction and wear performance, and cytotoxicity of additively manufactured zirconia-toughened alumina for dental applications[J]. *Composites, Part B. Engineering*, 250 (2023), 110459. doi:10.1016/j.compositesb.2022.110459
- Y. L. Chin, W. H. Tuan, Contribution of plastic deformation of Ti<sub>3</sub>SiC<sub>2</sub> to the crack deflection in the Al<sub>2</sub>O<sub>3</sub>/Ti<sub>3</sub>SiC<sub>2</sub> composites[J]. *Materials Science & Engineering A*, 2011, 528(7–8): 3270–3274. doi:10.1016/j.msea.2010.12.084.
- G. Pezzotti, H. Wolfgang, Müller, Strengthening mechanisms in Al<sub>2</sub>O<sub>3</sub>/SiC nanocomposites[J]. *Computational Materials Science*, 22 (2001) 3–4, 155–168. doi: 10.1016/S0927-0256(01)00185-9.
- L. T. Yan, W. J. Si, T. Xiong, T. H. Miao, The overview of Al<sub>2</sub>O<sub>3</sub>/SiC nanocomposites II-: Strengthening and toughening mechanism[J]. *Rare metal materials and engineering*, 2004, 33 (6): 10–13.
- Z. Q. Chen, N. S. Guo, L. G. Ji, L. R. X. Guo, C. H. Xu, Influence of CaF<sub>2</sub>@Al<sub>2</sub>O<sub>3</sub> on the friction and wear properties of Al<sub>2</sub>O<sub>3</sub>/Ti(C,N)/CaF<sub>2</sub>@Al<sub>2</sub>O<sub>3</sub> self-lubricating ceramic tool[J]. *Materials Chemistry and Physics*, 223 (2019), 306–310. doi:10.1016/j.matchemphys.2018.11.006
- C. Xue, D. Wang, J. J. Zhang, Wear Mechanisms and Notch Formation of Whisker-Reinforced Alumina and Sialon Ceramic Tools during High-Speed Turning of Inconel 718, *Materials*, 15 (2022) 11, 3860–3860. doi:10.3390/ma15113860
- J. L. Chai, Y. B. Zhu, Z. G. Wang, T. L. Shen, Y. W. Liu, L. J. Niu, S. F. Li, C. F. Yao, M. H. Cui, C. Liu, Microstructure and mechanical properties of SPS sintered Al<sub>2</sub>O<sub>3</sub>-ZrO<sub>2</sub>(3Y)-SiC ceramic composites, *Materials Science & Engineering, A. Structural Materials: Properties, Microstructure and Processing*, 781 (2020), 139197. doi:10.1016/j.msea.2020.139197
- Y. E. Eren, T. O. Ergüder, G. Kaya, I. Hacısalıhoğlu, B. Yay, F. Yıldız, Wear behavior of Ni-B coated-hard anodized Al7Si alloy and machining performance with ZrN ceramic film coated carbide tool[J]. *Surfaces and Interfaces*, 21 (2020), 100768. doi:10.1016/j.surfint.2020.100768
- S. Gustafsson, L. K. L. Falk, E. Lidén, E. Carlström, Alumina/silicon carbide composites fabricated via in situ synthesis of nano-sized SiC particles, *Ceramics International*, 35 (2009) 3, 1293–1296. doi:10.1016/j.ceramint.2008.05.013
- Wu Guangyong, Study on Nickel-coated hexagonal boron nitride self-lubricating ceramic tool and its properties, Shandong University, (2020). doi:10.27272/d.cnki.gshdu.2020.000487
- Y. B. Zhao, Z. Li, Y. Li, J. Q. Wu, Z. L. Gao, C. W. Wu, X. Y. Yu, M. Jin, G. Y. Wen, H. Zhou, Effect of ceramic particle shape on wear resistance mechanism of zirconia toughened alumina ceramic reinforced high chromium cast iron architectural composite[J]. *Ceramics International*, 50 (2024) 7, 11370–11378. doi:10.1016/j.ceramint.2024.01.037
- E. Martínez-Franco, J. Trejo-Camacho, C. Ma, S. Díaz de la Torre, A. I. García-Moreno, A. M. Benítez-Castro, G. Trapaga-Martínez, J. M. Alvarado-Orozco, J. Muñoz-Saldaña, Mechanical characterization by multiscale indentation of particle reinforced Nickel-Alumina metal matrix nanocomposites obtained by high-kinetic processing of ball milling and spark plasma sintering, *Journal of Alloys and Compounds*, 927 (2022), 166880. doi:10.1016/j.jallcom.2022.166880
- D. Firoozbakht, S. A. Sajjadi, H. Beygi, H. Sazegaran, Low-temperature pressureless sintering of Al<sub>2</sub>O<sub>3</sub>-SiC-Ni nanocermet in air environment, *Ceramics International*, 44 (2018) 15, 18156–18163. doi:10.1016/j.ceramint.2018.07.023
- H. Irshad, A. S. Hakeem, B. A. Ahmed, S. Ali, S. Ali, M. A. Ehsan, T. Laoui, Effect of Ni content and Al<sub>2</sub>O<sub>3</sub> particle size on the thermal and mechanical properties of Al<sub>2</sub>O<sub>3</sub>/Ni composites prepared by spark plasma sintering, *International Journal of Refractory Metals & Hard Materials*, 76 (2018), 25–32. doi:10.1016/j.ijrmhm.2018.05.010

- <sup>18</sup> Y. Wang, W. C. Sun, C. A. Wang, Y. Huang, J. M. Xu, Microstructure, friction, and wear properties of Ni-Al<sub>2</sub>O<sub>3</sub>-MoS<sub>2</sub> composite coatings, *International journal of applied ceramic technology*, 14 (2017) 5, 889–898. doi:10.1111/ijac.12744
- <sup>19</sup> Y. Fei, C. Huang, H. Liu, The Phase Composition and Mechanical Properties of Al<sub>2</sub>O<sub>3</sub>-TiN-TiC Ceramic Materials with Different Ni Content, *Journal of Ceramic Science and Technology*, 10 (2019) 2. doi:10.4416/JCST2019-00012
- <sup>20</sup> G. Q. Liu, S. X. Chen, Y. W. Zhao, Y. D. Fu, Y. J. Wang, Effect of Ti and its compounds on the mechanical properties and microstructure of B<sub>4</sub>C ceramics fabricated via pressureless sintering, *Ceramics international*, 47 (2021) 10, 13756–13761. doi:10.1016/j.ceramint.2021.01.237
- <sup>21</sup> M. X. Jing, X. Q. Shen, W. X. Li, D. H. Li, Effects of Ni-doping mode on microstructure and mechanical properties of alumina/Ni composites, *International Journal of Materials & Product Technology*, 34 (2009) 3, 342–351. doi:10.1504/IJMPT.2009.024666.
- <sup>22</sup> T. Feng, W. Zheng, W. G. Chen, Y. G. Shi, Y. Q. Fu, Enhanced interfacial wettability and mechanical properties of Ni@Al<sub>2</sub>O<sub>3</sub>/Cu ceramic matrix composites using spark plasma sintering of Ni coated Al<sub>2</sub>O<sub>3</sub> powders, *Vacuum: Technology Applications & Ion Physics: The International Journal & Abstracting Service for Vacuum Science & Technology*, 184 (2021) 1, 109938. doi:10.1016/j.vacuum.2020.109938
- <sup>23</sup> M. H. Nabbouh, R. Naghizadeh, F. Golestani-Fard, H. Rezaie, Processing and properties of Ni dispersed zirconia toughened alumina[J], *Journal of Ceramic Processing Research*, 9 (2017) 18, 621–627.
- <sup>24</sup> R. Yamanoglu, E. Karakulak, M. Zeren, Mechanical and wear properties of pre-alloyed molybdenum P/M steels with nickel addition, *Journal of Mining and Metallurgy Section B Metallurgy*, 48 (2012) 2, 251–258. doi:10.2298/JMMB111128026Y.
- <sup>25</sup> R. Z. M. Karakulak, Mechanical properties of hypoeutectic Al-Ni alloys with Al<sub>3</sub>Ni intermetallics, *Materials Testing*, 58 (2016) 2, 117–121. doi:10.3139/120.110825
- <sup>26</sup> J. T. Luo, S. Y. Luo, C. X. Zhang, Y. H. Xue, G. Q. Chen, Analysis of the intragranular microstructure in ceramic nanocomposites and their effect on the mechanical properties, *Journal of the American Ceramic Society*, 10 (2018) 11, 5151–5156. doi:10.1111/jace.15729
- <sup>27</sup> H. Awaji, S. M. Choi, E. Yagi, Mechanisms of toughening and strengthening in ceramic-based nanocomposites, *Mechanics of Materials*, 34 (2002) 7, 411–422. doi:10.1016/S0167-6636(02)00129-1
- <sup>28</sup> M. H. Nabbouh, R. Naghizadeh, F. Golestani-Fard, H. Rezaie, Processing and properties of Ni dispersed zirconia toughened alumina, *Journal of Ceramic Processing Research*, 18 (2017) 9, 621–627
- <sup>29</sup> R. O. Ritchie, Toughening materials: Enhancing resistance to fracture, *Philosophical Transactions of The Royal Society A Mathematical Physical and Engineering Sciences*, 379 (2021), 20200437. doi:10.1098/rsta.2020.0437
- <sup>30</sup> J. Tanska, P. Wieceński, M. Kukielski, J. Zygmuntowicz, P. Wieceńska, Coordination complexes as substitutes for metallic powders in ceramic-matrix-composites manufactured by aqueous colloidal processing: Enhanced fracture toughness and quantitative microstructure analysis, *Journal of the European Ceramic Society*, 44 (2024) 1, 341–352. doi:10.1016/j.jeurceramsoc.2023.08.059
- <sup>31</sup> T. F. Grigoreva, T. L. Talako, E. T. Devyatkina, S. V. Vosmerikov, S. V. Tsybulya, Mechanochemical Modification of Nickel Aluminide with Aluminum Oxide, *Russian journal of applied chemistry*, 95 (2022) 8, 1125–1128. doi:10.1134/S1070427222080055
- <sup>32</sup> A. Naseem, M. Aas, M. R. Lal, S. K. Kumar, G. Pallav, Correlation of structural and mechanical properties for Al-Al<sub>2</sub>O<sub>3</sub>/SiC hybrid metal matrix composites[J], *Journal of Composite Materials*, 55 (2021) 23, 3267–3280. doi:10.1177/00219983211011537
- <sup>33</sup> Q. Su, S. Zhu, Y. Bai, H. Ding, P. Di, Preparation and elevated temperature wear behavior of Ni doped WC-Al<sub>2</sub>O<sub>3</sub> composite, *International Journal of Refractory Metals & Hard Materials*, 81 (2019), 167–172. doi:10.1016/j.jrmhm.2019.03.005
- <sup>34</sup> B. Wang, H. Liu, H. T. Zhu, C. Z. Huang, B. Zhao, Y. Liu, Effect of Ni on mechanical behavior of Al<sub>2</sub>O<sub>3</sub>/(W,Ti)C ceramic tool materials at ambient and elevated temperatures, *Materials Research Express*, 6 (2019) 4, 045028. doi:10.1088/2053-1591/aafc06.
- <sup>35</sup> Y. Torres, J. M. Tarrago, D. Coureaux, E. Tarrés, B. Roebuck, P. Chan, M. James, B. Liang, M. Tillman, R. K. Viswanadham, K. P. Mingard, A. Mestra, L. Llanes, Fracture and fatigue of rock bit cemented carbides: Mechanics and mechanisms of crack growth resistance under monotonic and cyclic loading[J], *International Journal of Refractory Metals and Hard Materials*, 45 (2014), 179–188. doi:10.1016/j.jrmhm.2014.04.010
- <sup>36</sup> H. Duan, H. L. Mo, R. S. Qiu, X. Chen, Y. Liu, Effect of Ni Content on High-Temperature Oxidation Resistance of TiN-Ni Cermets, *Rare metal materials and engineering*, 49 (2020) 2, 595–599.
- <sup>37</sup> X. B. Zhang, H. Chen, G. C. Xiao, M. D. Yi, J. J. Zhang, Z. Q. Chen, Q. Lin, C. H. Xu, Alumina ceramic tool material with enhanced properties through the addition of bionic prepared nano SiC@graphene, *Ceramics International*, 49 (2023) 12, 19753–19765. doi:10.1016/j.ceramint.2023.03.093
- <sup>38</sup> A. Henniche, J. H. Ouyang, Z. G. Liu, Y. H. Ma, Z. G. Wang, M. Derradji, Effect of SiC addition on mechanical properties of hot-pressed Al<sub>2</sub>O<sub>3</sub>-GdAlO<sub>3</sub> ceramics with eutectic composition[J], *Ceramics International*, 44 (2018) 8, 9585–9592. doi:10.1016/j.ceramint.2018.02.182
- <sup>39</sup> J. Zhang, K. Su, Z. H. Wang, Q. K. Geng, H. S. Wang, J. X. Shen, E. X. Xu, F. Zhao, Z. T. Luo, X. H. Liu, Effect of Al(H<sub>2</sub>PO<sub>4</sub>)<sub>3</sub>/Zn/B<sub>4</sub>C doped resin on properties and microstructure of unfired Al<sub>2</sub>O<sub>3</sub>-C slide plate materials[J], *Ceramics International*, 48 (2021) 1, 472–480. doi:10.1016/j.ceramint.2021.09.123